ЖУРНАЛ СТРУКТУРНОЙ ХИМИИ

2017. Том 58, № 3 *Март – апрель* *С. 506 – 515*

UDC 541.6:547.021

EFFECTS OF HETEROATOMS ON THE ELECTRONIC, SENSOR, AND ADSORPTION PROPERTIES OF GRAPHENE

S. Amir Aslanzadeh

Technical Vocational University, Yaftabad, Tehran, Iran
E-mail: saeedamiraslanzadeh@hotmail.com

Received August, 25, 2015 *Revised — March, 29, 2016*

The effects of doping heteroatoms on the structure, electronic and adsorption properties of graphene are investigated using density functional theory calculations. Six different doped graphenes (with Al, B, Si, N, P, and S) are considered, and to obtain the interaction and adsorption properties, three sulfur-containing molecules (H_2S, SO_2, and thiophene) were interacted with selected graphenes. The adsorption energies (E_{ad}) in the gas phase and solvents show the exothermic interaction for all complexes. The maximum E_{ad} values are observed for aluminum doped graphene (AG) and silicon doped graphene (SiG), and adsorption energies in the solvent are not so different from those in the gas phase. NBO calculations show that the AG and SiG complexes have the highest $E^{(2)}$ interaction energies and simple graphene (G) and nitrogen doped graphene (NG) have the least $E^{(2)}$ energies. Population analyses show that doping heteroatoms change the energy gap. This gap changes more during the interaction and these changes make these structures useful in sensor devices. All calculated data confirm better adsorption of SO_2 by graphenes versus H_2S and thiophene. Among all graphenes, AG and then SiG are the best adsorbents for these structures.

DOI: 10.15372/JSC20170308

K e y w o r d s: graphene, heterodoping, sensor, adsorption.

INTRODUCTION

After the first isolation of graphene by mechanical exfoliation of graphite, it was found to be a special structure with promising properties [1]. Graphene has exhibited prominent properties in mechanics, electrics, and optics. It has a high charge carrier mobility and therefore, it is one of the best candidates for the next generation of electronic devices [2]. Graphene transfers electrons faster than silicon and this is another promising property to employ it in electronic devices. Because of these high potencies, graphene have been employed as a new material in many systems such as semiconductors, fuel cells, sensors, ion transfer, selective membrane, and water desalination [3—8]. Moreover, the doping of graphene by different heteroatoms could be interesting because it will be another method to modify its properties and produce new materials with new abilities.

During recent years, many methods have been developed to produce simple and doped nanostructures, such as graphenes, fullerenes, and carbon nanotubes [9—11]. However, the doping of graphene has been studied less than the doping of nanotubes or fullerenes, despite the special properties and potencies obtainable from its doping. In this line, doped graphenes could be used in gas sensor devices and they could open new horizons in this area [12]. To get better insight into the sensor properties, density functional theory (DFT) calculations have been mostly used because they could calculate the electronic properties and determine the adsorption energies of various molecules on the surface of

doped nanostructures [13—15]. Moreover, by DFT calculations, the P and N doping effects on the properties of graphene have been investigated [16]. Despite the huge number of experimental and theoretical investigations of the properties and applications of simple graphenes [17—23], only few reports could be observed regarding doped graphenes [24, 25], and many aspects of these new materials have been unknown so far. More importantly, by reviewing the literature, any systematic reports related to the effects of doping graphene with different heteroatoms on its properties, abilities and applications have not been observed while a similar study on carbon nanotubes has been published [26]. In this context, the adsorption and sensor properties and interaction abilities of these doped systems could be examined by employing some sample molecules as adsorbates. Therefore, we have decided to perform a comprehensive study on the properties of doped graphenes with different heteroatoms and adsorption of some molecules (H_2S, SO_2, and thiophene) on their surface to compare their abilities. Moreover, the molecular properties of parent structures, the nature of these interactions, interaction energies and sensor properties should be considered.

In this work, the molecular and electronic properties of simple and six doped graphene (with Al, B, Si, N, P, and S) were investigated using DFT calculations. In addition, their abilities in the adsorption of different sulfur-containing pollutants (H_2S, SO_2, and thiophene) have been compared. Therefore, adsorption energies, optimized parameters, and the molecular orbital properties, such as HOMO-LUMO energies, their energy gap (E_g) and density of states (DOS) plots, were calculated using DFT and the interaction parameters and atomic charges were studied using NBO calculations. The computational details of this study and the results are presented.

METHODS

Gaussian 09 [27] was employed to perform all calculations. These calculations were carried out using DFT at the ωB97XD/6-31+G* level of theory. DFT has showed high abilities in the calculation of molecular [28] and spectral [29, 30] properties of chemical structures, comparable with MP2 methods [31, 32], including their acceptable results in the prediction of thermodynamic and kinetic properties of chemical phenomena [33—35]. Moreover, among various DFT methods, ωB97XD have been designed as the best DFT code to interpret the intermolecular interactions. Chai and Head-Gordon developed the ωB97XD code based on the former ωB97X method by applying some empirical correction for binary atomic dispersion [36—38].

In this work, all the structures were optimized without any symmetric restriction or pre-defined conformational structures. Moreover, to consider solvation effects, the free energy of solvation (using water as a solvent) was calculated for each molecule by the SCRF keyword using Tomasi′s polarized continuum (PCM) model [39]. Since the adsorption energy is one of the parameters reported here, equation (1) computes the energy of the non-covalent interaction of complexes in both gas and solvent phases

$$\Delta E_{ads} = E_{complex} - (E_{adsorbent} + E_{adsorbate}). \quad (1)$$

To obtain more information related to these intramolecular interactions, NBO analyses of all structures were performed using the NBO [40] program as implemented in the Gaussian program package. The density of state (DOS) plot was also obtained from the GaussSumm program [41] to investigate the electronic and sensor properties. Finally, reactivity parameters were calculated for all structures using the Koopmans theorem [42] and therefore, the chemical potential (μ), the chemical hardness (η), the global softness (S), and the electrophilicity index (ω) were computed for all complexes from the equations (2)—(5).

$$\mu = (E_{LUMO} + E_{HOMO})/2, \quad (2)$$

$$\eta = (E_{LUMO} - E_{HOMO})/2, \quad (3)$$

$$S = 1/\eta, \quad (4)$$

$$\omega = \mu^2/2\eta. \quad (5)$$

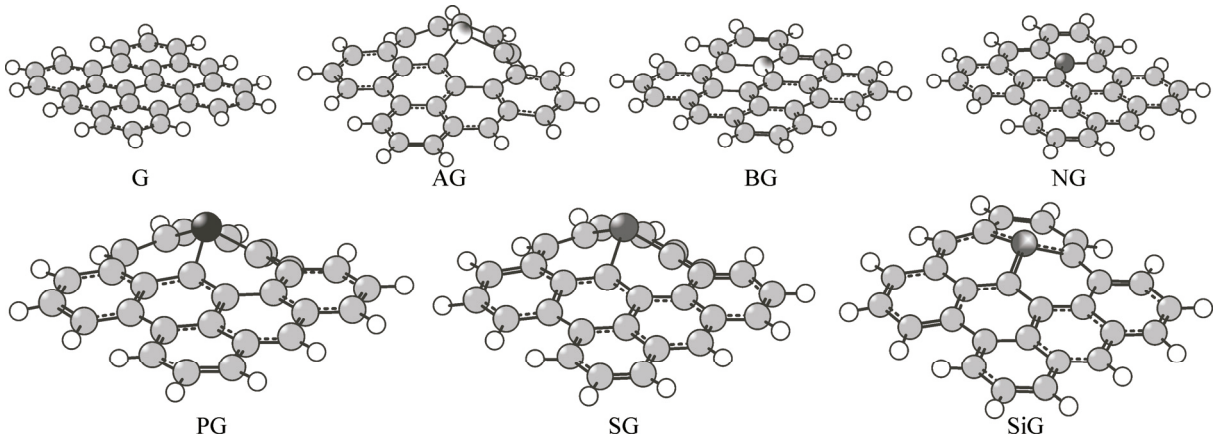

Fig. 1. Optimized structures of simple and doped graphenes employed in this work

RESULTS AND DISCUSSION

Optimized parameters. We have started with one simple graphene (simply named G) whose all edges were saturated with hydrogen. This structure was optimized and by doping six heteroatoms into its structure six graphenes doped with one aluminum atom (AG), boron (BG), nitrogen (NG), phosphorus (PG), sulfur (SG), and silicon (SiG) were obtained (totally, 7 structures). These structures were first optimized at the ωB97XD/6-31+G* level of theory (as described above, all calculations were performed using this method and basis set) and the optimized structures were used to preform next calculations and extract the molecular parameters and energies. Fig. 1 depicts the optimized structures of these molecules.

Further, three adsorbates (H_2S, SO_2, and thiophene, named generally as M) were selected as three important small molecules. The structures of these adsorbates were optimized and then placed on the surface of each adsorbent in various configurations to obtain the best configuration of each adsorbent—adsorbate complex (simply named as complex). These most stable complexes were used in the next calculations to extract the molecular parameters and energies. The optimized structures of these complexes (21 complexes) are shown in Fig. 2 and the important molecular parameters of these complexes and initial structures (simple and doped graphenes) are listed in Table 1.

Table 1

Important molecular parameters of adsorbents and their complexes

Parameter	Simple	With H_2S		With SO_2		With thiophene	
	C—X (Av.)[a]	C—X (Av.)[a]	G—M[b]	C—X (Av.)[a]	G—M[b]	C—X (Av.)[a]	G—M[b]
G	1.429	1.430	2.827	1.429	2.859	1.427	3.162
AG	1.877	1.897	2.616	1.960	1.819	1.896	2.473
BG	1.514	1.513	2.708	1.512	2.907	1.515	3.142
NG	1.417	1.415	2.771	1.401	2.558	1.415	3.128
PG	1.841	1.839	2.800	1.859	1.531	1.840	3.187
SG	1.848	1.848	2.676	1.837	2.923	1.846	2.902
SiG	1.769	1.768	2.751	1.840	1.741	1.765	3.041

[a] This distance shows the average values of three C—X bond lengths.

[b] This parameter is related to the minimum distance between graphenes (G) and small molecules (M).

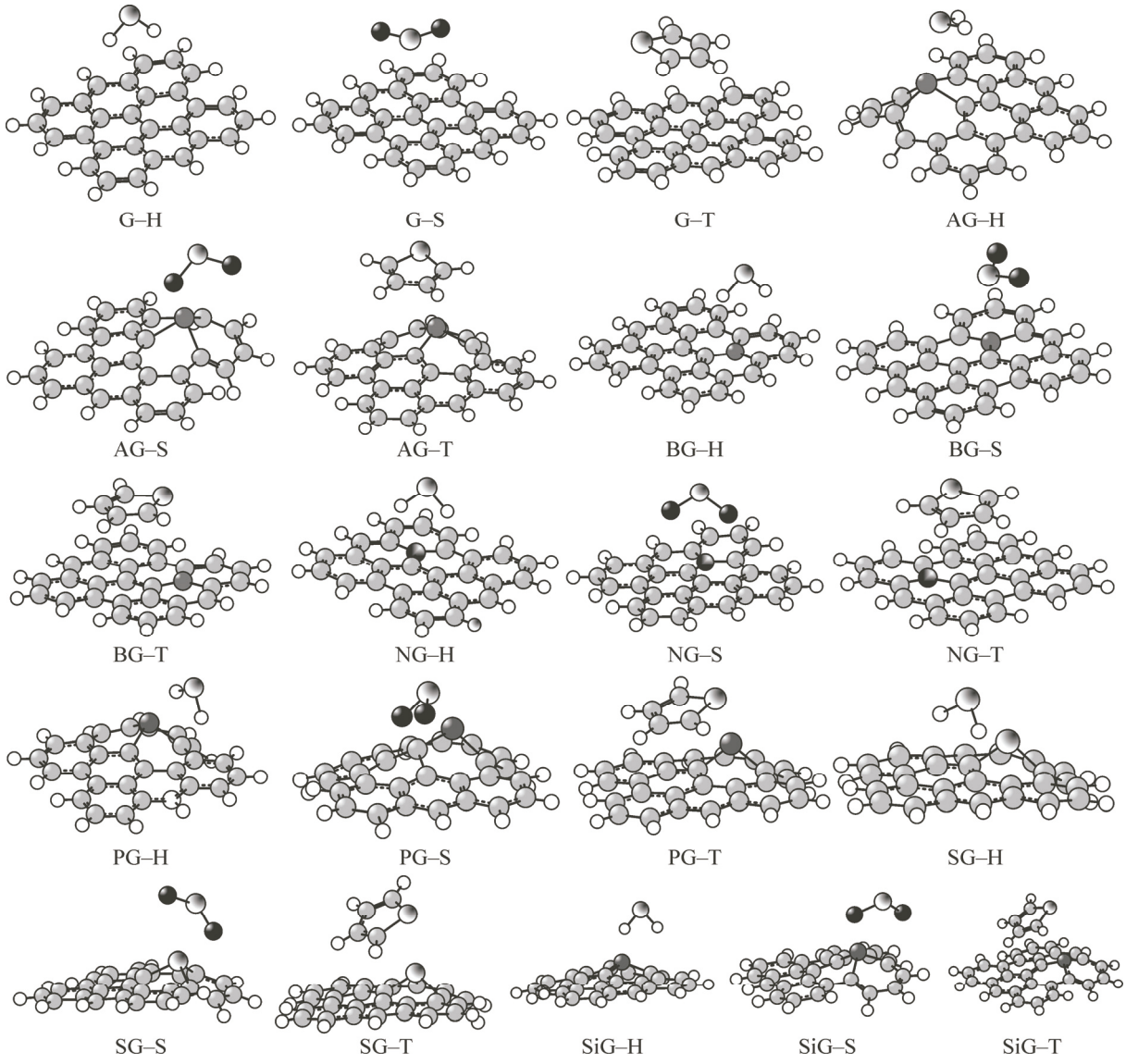

Fig. 2. Optimized structures for all complexes of graphenes with H_2S, SO_2, and thiophene

In Table 1, C—X values show the average values of three C—X bond lengths in graphenes are reported for all adsorbents and complexes. Moreover, G—M values are related to the minimum distance between graphenes (G) and small molecules (M) reported only for complexes. According to the calculated values, C—X distances in G, BG, and SG are nearly equal to C—X distances in their related complexes with M (H_2S, SO_2, and thiophene) while in AG, PG, NG and SiG, this distance changes meaningfully in their complexes versus the initial structures. The maximum variation of the C—X distance was observed in AG, with these values for AG, AG—H_2S, AG—SO_2, and AG—thiophene being respectively 1.877, 1.897, 1.960, and 1.896 Å. It should be noticed that in most complexes, the C—X distance increased versus that in the initial structure while in all SiG complexes, this value decreased versus that in SiG alone.

The G—M distance is related to the atomic size of adjacent atoms and when the adjacent atoms are equal it could be related to the strength of interactions. By averaging all G—M distances in various graphenes with each M, the minimum distance is calculated for complexes with SO_2 (2.246 Å), then H_2S (2.720 Å), and then thiophene (2.979 Å). These values show that the complexes of our structures with SO_2 could be the strongest complexes. In addition, by a comparison of different graphenes, the

Table 2

Interaction energies (ΔE_{ad}) *of all nanostructures with* H_2S, SO_2, *and thiophene in gas and solvent* (*water*, *using* PCM *model*)

Parameter	With H_2S		With SO_2		With thiophene	
	E_{ad}(G)	E_{ad}(solv)	E_{ad}(G)	E_{ad}(solv)	E_{ad}(G)	E_{ad}(solv)
G	–5.37	–4.09	–10.01	–9.70	–9.54	–8.35
AG	–15.91	–16.14	–74.75	–76.11	–18.06	–18.48
BG	–6.37	–4.91	–10.82	–10.53	–9.53	–8.37
NG	–5.22	–3.87	–19.02	–27.94	–10.74	–9.39
PG	–5.94	–4.53	–28.03	–24.79	–9.59	–8.39
SG	–6.76	–5.11	–5.87	–4.65	–9.38	–7.77
SiG	–6.12	–4.46	–40.04	–52.40	–10.08	–8.77

average G—M distances (for all three complexes of each structure) are in this order: AG < PG < SiG < < NG < SG < BG < G. To interpret these values, it should be noticed that Al, S, Si, and P are in the third row of periodic tables and normally have larger atomic radii than C, B, and N atoms. With regard to this fact, the values show that aluminum-doped graphenes have the highest abilities in the adsorption of H_2S, SO_2, and thiophene while simple graphene is the worse adsorbent for these molecules (only by the G—M distances).

Adsorption energies (in gas and solvent). The possibility of the adsorption process and the strengths of interactions between graphenes and our adsorbates could be obtained from the adsorption energies (E_{ad}, using Eq. (1)). These energies were calculated for all complexes (7 adsorbent and 3 adsorbate, totally 21 complexes) in both gas phase and solvent (water) and the results were listed in Table 2. According to the Table 2 data, all adsorption energies are negative and it could be concluded that our adsorbates (H_2S, SO_2, and thiophene) have the exothermic and favorable interaction with graphenes (simple and doped). A comparison of the gas phase and solvent adsorption values shows that these values are very close with minor differences. Interestingly, the majority of adsorption processes in the gas phase are more favorable than those in the solvent. There are only six exceptions related to these values; i.e. H_2S adsorption by AG, SO_2 adsorption by NG and SiG, and thiophene adsorption by AG. In these cases, the adsorption processes in the solvent are slightly more favorable than those in the gas phase.

Among the studied adsorbates (H_2S, SO_2, and thiophene), the E_{ad} values for SO_2 are the most negative values and the least negative value is for H_2S. Therefore, most graphenes have a more favorable interaction with SO_2 and a less favorable interaction with H_2S in comparison with their interaction with thiophene. Another comparison could be made between the abilities of various simple and doped graphenes that help scientists to make choice between them when they deal with the real problem. According to the calculated values and on average, the order of adsorption abilities (versus our adsorbates), extracted from the E_{ad} values, are: AG > SiG > PG > NG > BG > G > SG. It shows that AG and then SiG are the best adsorbents among doped graphenes and most doped graphenes have better interactions as compared to simple graphene. This order is nearly the same as the order obtained from the molecular parameters and discussed above (only the orders of BG and NG changed). In addition, the E_{ad} values of AG are numerously greater than those of the other graphenes and the adsorption energies of SG, BG, and G are close.

NBO calculations. From the natural bond orbital calculations, two important parameters, atomic charges, and interaction energies between different parts of the structures (second order perturbation energies), could be obtained with high accuracy. In this work, the most important atomic charges were extracted from the NBO calculations and the results were listed in Table 3. To make a better comparison, the NBO atomic charges of discrete adsorbents (columns 2 and 3 of the upper part of Table 3) and adsorbates (the first row of data in the down part of Table 3) were listed in this table. In Table 3, the average atomic charges of three carbon atoms connected to the doped heteroatom were reported as the

Table 3

Selected NBO *atomic charges of adsorbates alone and in complexes with selected models of* CNT, SCNT, *and* S2CNT

The charges of graphene part of molecule	G alone		G—H_2S		G—SO_2		G—thiophene	
	C(Av)[a]	X[b]	C(Av)[a]	X[b]	C(Av)[a]	X[b]	C(Av)[a]	X[b]
G	–0.011	–0.002	–0.032	–0.030	–0.035	–0.018	–0.009	–0.003
AG	–0.560	1.631	–0.558	1.584	–0.427	1.713	–0.586	1.752
BG	–0.342	0.635	–0.350	0.606	–0.346	0.546	–0.341	0.649
NG	0.214	–0.330	0.212	–0.328	0.250	–0.27	0.219	–0.324
PG	–0.294	0.912	–0.293	0.893	–0.225	0.901	–0.291	0.911
SG	–0.204	0.839	–0.203	0.852	–0.190	0.831	–0.200	0.854
SiG	–0.511	1.476	–0.525	1.516	–0.440	1.912	–0.536	1.557

The charges of adsorbate part of molecules	G—H_2S		G—SO_2		G—thiophene	
	S	Y(Av)[d]	S	Y(Av)[d]	S	Y(Av)[d]
Simple molecule[c]	–0.340	0.170	1.286	–0.643	0.358	–0.416
G	–0.349	0.173	1.219	–0.696	0.353	–0.416
AG	–0.258	0.227	0.953	–0.821	0.448	–0.416
BG	–0.355	0.177	1.280	–0.696	0.366	–0.415
NG	–0.348	0.173	0.845	–0.850	0.347	–0.418
PG	–0.351	0.169	0.874	–0.607	0.358	–0.417
SG	–0.362	0.178	1.199	–0.692	0.344	–0.417
SiG	–0.347	0.178	0.691	–0.850	0.352	–0.417

[a] This value is the average of atomic charges of three carbon atoms connected to the doped heteroatom.

[b] This value is the charge of doped heteroatom in doped graphenes. For G, this is the charge of carbon atom near to the adsorbate.

[c] Small molecule is implicated to H_2S, SO_2 and thiophene.

[d] Y the average of atomic charges of two hydrogen atoms in H_2S, two oxygen atoms in SO_2 and C1 and C5 in thiophene.

C(Av) charge, the doped heteroatom charge in doped graphenes was reported as the X charge (for undoped graphene, G, this is the charge of a carbon atom near to the adsorbate), the sulfur atom charge in H_2S, SO_2, and thiophene was reported as the S charge, and the average atomic charges of two hydrogen atoms in H_2S, two oxygen atoms in SO_2 and C1 and C5 in thiophene were reported as the Y charge. The variation of adsorbent or adsorbate charges in each complex versus their initial charges is a criterion of charge transfer between them in the complex. In graphene complexes, small charge transfer (less than 0.024) could be observed and the maximum charge alteration is related to the G—SO_2 complex. In the complexes of doped graphenes with H_2S and SO_2, the maximum charge transfer could be observed in SiG complexes. Moreover, for complexes with thiophene, the maximum charge transfer belongs to AG. Therefore, in accordance with the previous results, AG and SiG are the best adsorbents for sulfur-containing adsorbates. Moreover, the charge transfer values in complexes with SO_2 are the largest values, which shows that this molecule has a more effective interaction with simple and doped graphenes.

Another data calculated by the NBO method, the most important acceptor-donor interactions ($E^{(2)}$ energies), extracted from the calculations, are listed in Table 4. For each complex, three interactions with the highest $E^{(2)}$ values were reported in order. Moreover, the sum of these three $E^{(2)}$ values for each complex was listed in the last column. Among various graphenes, AG and SiG complexes have

Table 4

Strongest second order perturbation energies (kcal/mol) *for the donor—acceptor transaction of all models*

Parameter	Donor	Acceptor	$E^{(2)}$	Donor	Acceptor	$E^{(2)}$	Donor	Acceptor	$E^{(2)}$	Sum[a]
G—H	Π_{C-C}	σ^*_{S-H}	0.68	Π_{C-C}	σ^*_{S-H}	0.57	Π_{C-C}	σ^*_{S-H}	0.14	1.39
G—S	Π_{C-C}	LP^*_S	0.81	LP_O	Π^*_{C-C}	0.80	LP^*_S	Π^*_{C-C}	0.69	2.30
G—T	Π^*_{C-C}	Π^*_{C-C}	1.69	Π^*_{C-C}	Π^*_{C-C}	0.88	Π_{C-C}	Π^*_{C-C}	0.45	3.02
AG—H	LP_S	LP^*_{Al}	25.78	LP_S	LP^*_{Al}	12.98	LP_S	σ^*_{C-Al}	5.24	44.00
AG—S	LP_O	LP^*_{Al}	48.75	LP^*_{Al}	σ^*_{S-O}	34.43	LP_O	LP^*_{Al}	20.41	103.59
AG—T	σ_{C-C}	LP^*_{Al}	11.35	σ_{C-C}	LP^*_{Al}	8.56	Π^*_{C-C}	LP^*_{Al}	7.11	27.02
BG—H	Π_{C-B}	σ^*_{S-H}	1.00	Π_{C-C}	σ^*_{S-H}	0.51	σ_{S-H}	Π^*_{C-B}	0.40	1.91
BG—S	LP^*_S	LP^*_B	8.45	LP_S	LP^*_B	3.05	Π_{C-C}	LP^*_S	1.74	13.24
BG—T	Π^*_{C-C}	Π^*_{C-C}	0.61	LP_S	Π^*_{C-B}	0.47	Π^*_{C-C}	Π^*_{C-C}	0.43	1.51
NG—H	Π_{C-C}	σ^*_{S-H}	0.22	Π^*_{C-C}	σ^*_{S-H}	0.16	Π_{C-C}	σ^*_{S-H}	0.14	0.52
NG—S	LP_O	Π^*_{C-C}	1.50	LP_O	Π^*_{C-C}	0.57	LP_O	Π^*_{C-C}	0.56	2.63
NG—T	Π^*_{C-C}	Π^*_{C-C}	0.81	Π^*_{C-C}	Π^*_{C-C}	0.61	Π^*_{C-C}	Π^*_{C-C}	0.58	2.00
PG—H	LP_P	σ^*_{S-H}	1.90	Π_{C-C}	σ^*_{S-H}	0.33	σ_{S-H}	σ^*_{C-P}	0.29	2.52
PG—S	LP_O	σ^*_{C-C}	2.20	σ_{C-C}	σ^*_{S-O}	1.87	σ^*_{S-O}	Π^*_{C-C}	1.65	5.72
PG—T	Π^*_{C-C}	Π^*_{C-C}	1.47	Π^*_{C-C}	Π^*_{C-C}	1.02	Π^*_{C-C}	Π^*_{C-C}	0.39	2.88
SG—H	Π_{C-C}	σ^*_{S-H}	1.87	Π^*_{C-C}	Π^*_{C-C}	0.21	σ_{C-C}	RY^*_H	0.18	2.26
SG—S	LP_S	LP^*_S	3.35	LP^*_S	LP_C	1.32	LP_O	Π^*_{C-C}	0.99	5.66
SG—T	Π_{C-C}	Π^*_{C-C}	0.54	Π_{C-C}	σ^*_{C-H}	0.41	LP_C	Π^*_{C-C}	0.40	1.35
SiG—H	LP_S	Π^*_{C-Si}	1.23	Π_{C-C}	σ^*_{S-H}	1.07	Π_{C-C}	σ^*_{S-H}	0.54	2.84
SiG—S	LP_O	LP^*_{Si}	212.56	σ^*_{S-O}	LP^*_{Si}	105.19	LP_O	LP^*_{Si}	33.16	350.91
SiG—T	LP_S	Π^*_{C-Si}	4.67	Π^*_{C-Si}	Π^*_{C-C}	2.24	LP_S	Π^*_{C-Si}	0.94	7.85

[a] This is the sum of three $E^{(2)}$ values listed in the same row.

the highest $E^{(2)}$ perturbation energies and PG complexes occupy the third rank in this order and their $E^{(2)}$ values are larger than those for BG (fourth rank), SG (fifth rank), G (sixth rank), and NG (last rank) complexes. Comparing the $E^{(2)}$ values of adsorbates, we see that the largest values belong to SO_2 complexes; thiophene and H_2S complexes have the least $E^{(2)}$ values (on average). These results match the previous data regard to the best adsorbates and adsorbents. A consideration of the nature of interacting orbitals shows that both adsorbent and adsorbate play the role of an electron donor and this electron exchange is a mutual process between two parts of each complex. This observation explains why sometimes we have a strong interaction while the net charge transfer is small.

Population analyses and DOS plots. To complete this work, the HOMO-LUMO band gaps and reactivity parameters were calculated by molecular orbital population analyses and the results are shown in Table 5. Moreover, in order to characterize the doping effect on the electronic properties of graphene, the density of state (DOS) plots for doped and undoped graphenes were depicted in Fig. 3. The order of energy gaps between HOMO and LUMO (E_g,) of various graphenes is: PG (0.205 eV) > > AG (0.203 eV) > NG (0.199 eV) > BG (0.184 eV) > G (0.180 eV) > SiG (0.179 eV) >SG (0.164 eV). Interestingly, except SiG and SG, the band gap of graphene increased with doping by heteroatoms,

Table 5

Energies of HOMO, LUMO *levels*, *energy gaps* (E_g), *chemical potential* (μ), *chemical hardness* (η), *global softness* (*S*) *and electrophilicity index* (ω) *for* CNTS, SCNTs, *and* S2CNTs. *All energy values are in the* eV *scale*

Parameter	E_{HOMO}	E_{LUMO}	E_g	μ	η	*S*	ω
G	–0.220	–0.041	0.180	–0.130	0.090	11.137	0.095
G—H	–0.226	–0.047	0.180	–0.137	0.090	11.137	0.104
G—S	–0.229	–0.068	0.161	–0.148	0.080	12.441	0.137
G—T	–0.220	–0.041	0.179	–0.130	0.090	11.150	0.095
AG	–0.223	–0.021	0.203	–0.122	0.101	9.868	0.073
AG—H	–0.219	–0.005	0.214	–0.112	0.107	9.340	0.058
AG—S	–0.254	–0.084	0.170	–0.169	0.085	11.755	0.169
AG—T	–0.214	–0.004	0.210	–0.109	0.105	9.519	0.057
BG	–0.228	–0.043	0.184	–0.135	0.092	10.857	0.100
BG—H	–0.233	–0.050	0.183	–0.142	0.091	10.953	0.110
BG—S	–0.235	–0.073	0.163	–0.154	0.081	12.298	0.146
BG—T	–0.227	–0.042	0.185	–0.135	0.093	10.799	0.098
NG	–0.196	0.003	0.199	–0.097	0.100	10.048	0.047
NG—H	–0.201	–0.002	0.200	–0.102	0.100	10.018	0.052
NG—S	–0.201	–0.058	0.143	–0.129	0.071	14.016	0.117
NG—T	–0.195	0.004	0.199	–0.096	0.100	10.038	0.046
PG	–0.222	–0.017	0.205	–0.120	0.103	9.746	0.070
PG—H	–0.229	–0.024	0.205	–0.126	0.103	9.744	0.078
PG—S	–0.248	–0.023	0.225	–0.136	0.112	8.889	0.082
PG—T	–0.221	–0.016	0.205	–0.119	0.103	9.750	0.069
SG	–0.197	–0.033	0.164	–0.115	0.082	12.176	0.081
SG—H	–0.204	–0.038	0.166	–0.121	0.083	12.075	0.088
SG—S	–0.204	–0.085	0.119	–0.145	0.059	16.852	0.176
SG—T	–0.198	–0.033	0.165	–0.115	0.082	12.144	0.081
SiG	–0.222	–0.042	0.179	–0.132	0.090	11.150	0.097
SiG—H	–0.226	–0.046	0.180	–0.136	0.090	11.140	0.103
SiG—S	–0.211	–0.099	0.112	–0.155	0.056	17.786	0.214
SiG—T	–0.220	–0.041	0.179	–0.130	0.089	11.178	0.095

especially P, Al, and N. The energy gap for SiG is nearly the same as that for G. However, the doping with sulfur atoms intensively reduces the energy gap, which makes SG a useful doped graphene with different properties.

Fig. 3 shows that SG has the best connectivity and PG has the worse connectivity in conducting bonds. Moreover, the connectivity of states (in both conductive and valence bonds) are different in all structures and in most doped graphenes; a better connectivity could be observed as compared to simple graphene. It should be noticed that this work presents graphenes doped with only one heteroatom and by doping with more than one heteroatom, E_g will decrease more, which shows that the conductivities of these structures could be controlled by the number of doped atoms.

The data listed in Table 5 show that in each adsorbent structure, the interaction with adsorbates changes its band gap. This property makes simple and doped graphenes useful as sensors for H_2S, SO_2, and thiophene. Since SO_2 was shown to have the strongest interaction with graphenes, its effect on E_g values is more than that of H_2S and thiophene. Doping of graphene with a heteroatom affects both E_{HOMO} and E_{LUMO} energies. A comparison of chemical potential (μ) values shows an increase in the

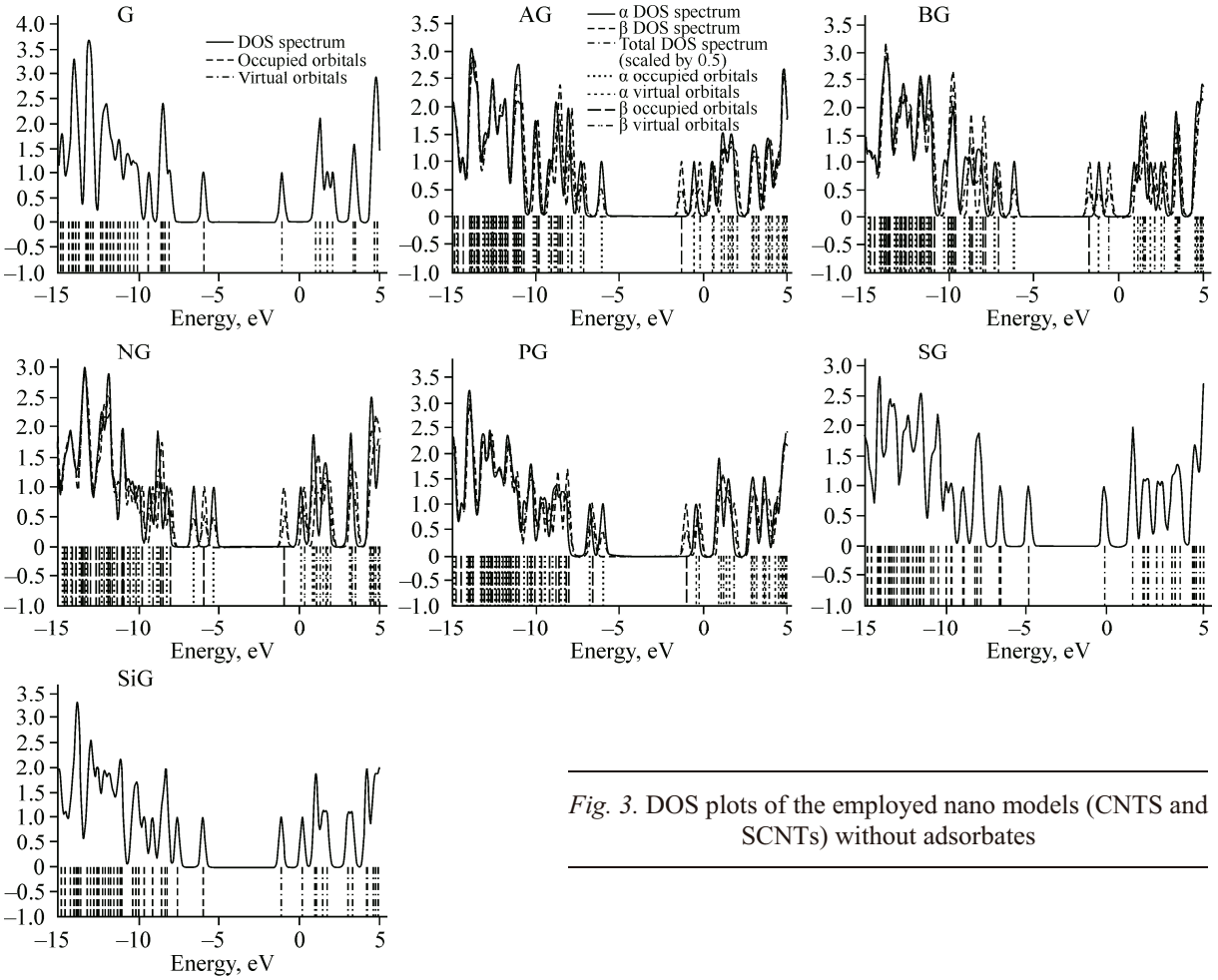

Fig. 3. DOS plots of the employed nano models (CNTS and SCNTs) without adsorbates

chemical potential of doped graphenes as compared to simple grapheme, except for BG, and the highest chemical potential was calculated for NG (–0.097 versus –0.130 for G). Moreover, the interaction with adsorbate, mostly decreases the chemical potential of adsorbent to more negative values. In this line, evidently, SO_2 complexes have the most intense effects on these properties. The chemical hardness (η) and global softness (S) values are related to E_g values and are not discussed more in this report. The order of the final values of this table, the electrophilicity index (ω), for various adsorbents is: BG > SiG > G < SG > AG > PG > NG. It could be observed that the doping or the dopant nature has no meaningful effect on the electrophilicity index. In addition, in all graphenes, complexation with SO_2 greatly increases the electrophilicity index while complexation with H_2S increases the electrophilicity index insignificantly (with one exception), and complexation with thiophene decreases the electrophilicity indexes.

CONCLUSIONS

Using DFT calculations, the abilities of simple and doped graphenes (with Al, B, Si, N, P, and S) in the interaction with three sulfur-containing molecules (H_2S, SO_2, and thiophene) have been compared to determine the effects of doping heteroatoms on their structures and properties. These interactions could be used in sensor, adsorption, and chemical reactions. To reach these purposes, in addition to the evaluation of important molecular parameters and atomic charges, the adsorption energies (in the gas form and water as asolvent) were calculated for all complexes. These values show that our adsorbates (H_2S, SO_2, and thiophene) have an exothermic interaction with simple and doped graphenes and the maximum E_{ad} values were observed for AG and SiG. By a simple comparison between the gas phase and solvent adsorption values it is shown that these values are very close with small differences.

Moreover, NBO calculations were employed to obtain the interaction energies ($E^{(2)}$) between various adsorbents and adsorbates. Among various graphenes, AG and SiG complexes have the highest $E^{(2)}$ perturbation energies and G and NG have the least adsorption energies. Population analyses were used to depict DOS plots and determine energy gaps and reactivity parameters. The observation of these values indicates that the doping by heteroatoms may increase or decrease the energy gap values. Moreover, the change in the energy gaps of the complexes (versus the initial adsorbent) shows that these structures could be used in sensor devices. The comparison of the chemical potential (μ) values reveals an increase in the chemical potential of doped graphenes. except BG (that has the least chemical potential) from that of simple grapheme, and the highest chemical potential was calculated for NG. All calculations show the better adsorption of SO_2 by graphenes versus H_2S and thiophene, and among all graphenes, AG and then SiG have the strongest interactions.

REFERENCES

1. *Lammert P.E., Crespi V.H.* // Phys. Rev. B. – 2000. – **61**. – P. 7308 – 7311.
2. *Karlicky F., Zboril R., Otyepka M.* // J. Chem. Phys. – 2012. – **137**. – P. 34709 – 34712.
3. *Rani P., Jindal V.K.* // RSC Adv. – 2013. – **3**. – P. 802 – 812.
4. *Castro E.V., Novoselov K.S., Morozov S.V. et al.* // Phys. Rev. Lett. – 2007. – **99**. – P. 216802 – 216805.
5. *Yang X., Wang Y., Huang X.V. et al.* // J. Mater. Chem. – 2011. – **21**. – P. 3448 – 3454.
6. *Ohern S.C., Boutilier M.S.H., Idrobo J.C. et al.* // Nano Lett. – 2014. – **14**. – P. 1234 − 1241.
7. *Sun P., Zhu M., Wang K. et al.* // ACS Nano. – 2013. – **7**. – P. 428 – 437.
8. *Tanugi D.C., Grossman J.C.* // Nano Lett. – 2012. – **12**. – P. 3602 − 3608.
9. *Koos A.A., Nicholls R.J., Dillon F. et al.* // Carbon. – 2012. – **50**. – P. 2816 – 2823.
10. *Liu J., Liu H., Zhang Y. et al.* // Carbon. – 2011. – **49**. – P. 5014 – 5021.
11. *Monteiro F.H., Larrude D.G., Maia da Costa M.E.H. et al.* // J. Phys. Chem. C. – 2012. – **116**. – P. 3281 – 3285.
12. *Yuan W., Shi G.J.* // Mater. Chem. A. – 2013. – **1**. – P. 10078 – 10091.
13. *Hassani F., Tavakol H.* // Sens. Actuators B. – 2014. – **196**. – P. 624 – 630.
14. *Tavakol H., Hassani F.* // Struct. Chem. – 2015. – **26**. – P. 151 – 158.
15. *Tavakol H., Mollaei-Renani A.* // Struct. Chem. – 2014. – **25**. – P. 1659 – 1667.
16. *Garcia A.L.E., Baltazar S.E., Romero A.H. et al.* // J. Comput. Theor. Nanosci. – 2008. – **5**. – P. 221 – 229.
17. *Shi G., Ding Y., Fang H.J.* // Comput. Chem. – 2012. – **33**. – P. 1328 – 1337.
18. *Anota E.C., Juarez A.R., Castro M. et al.* // J. Mol. Model. – 2013. – **19**. – P. 321 – 328.
19. *Kishi H., Tani M., Sakaue M. et al.* // J. Vac. Soc. Jpn. – 2012. – **55**. – P. 198 – 203.
20. *Ayala I.G., Cordero N.A.* // J. Nanopart. Res. – 2012. – **14**. – P. 1071 – 1079.
21. *Rudenko A.N., Keil F.J., Katsnelson M.I. et al.* // Phys. Rev. B. – 2012. – **86**. – 075422.
22. *Mirzaei M., Yousefi M.* // Superlattices Microstruct. – 2013. – **52**. – P. 1 – 7.
23. *Ambrosetti A., Silvestrelli P.L.* // J. Phys. Chem. C. – 2011. – **115**. – P. 3695 – 3702.
24. *Zhang L., Niu J., Dai L. et al.* // Langmuir. – 2012. – **28**. – P. 7542 – 7550.
25. *Gu X., Yang Y., Hu Y. et al.* // RSC Adv. – 2014. – **4**. – P. 63189 – 63199.
26. *Wang Y.L., Su K.H., Zhang J.P.* // Adv. Mater. Res. – 2012. – **463**. – P. 1488 – 1492.
27. *Frisch M.J., Trucks G.W., Schlegel H.B. et al.* Gaussian 09, Revision A.1, Gaussian, Inc., Wallingford CT. – USA, 2009.
28. *Tavakol H.* // THEOCHEM. – 2010. – **954**. – P. 16 – 21.
29. *Javanshir Z., Mehrani K., Ghammamy S. et al.* // Bull. Korean Chem. Soc. – 2008. – **2**. – P. 1464 – 1466.
30. *Tavakol H., Esfandyari M., Taheri S. et al.* // Spectrochim. Acta A. – 2011. – **79**. – P. 574 – 582.
31. *Johnson B.G., Gill P.M.W., Pople J.A.* // J. Chem. Phys. – 1993. – **98**. – P. 5612 – 5618.
32. *Bauschlicher C.W., Partridge H.T.* // Chem. Phys. Lett. – 1995. – **240**. – P. 533 – 540.
33. *Tavakol H., Hadadi T., Roohi H.* // J. Struct. Chem. – 2012. – **53**. – P. 649 – 658.
34. *Tavakol H.* // Int. J. Quantum Chem. – 2011. – **111**. – P. 3717 – 3724.
35. *Tavakol H.* // Mol. Simul. – 2010. – **36**. – P. 391 – 402.
36. *Chai J.D., Head-Gordon M.* // Phys. Chem. Chem. Phys. – 2008. – **10**. – P. 6615 – 6620.
37. *Antony J., Grimme S.* // Phys. Chem. Chem. Phys. – 2006. – **8**. – P. 5287 – 5293.
38. *Jurecka P., Cerny J., Hobza P. et al.* // J. Comput. Chem. – 2007. – **28**. – P. 555 – 569.
39. *Mietrus S., Scrocco E.* // J. Chem. Phys. – 1981. – **55**. – P. 117 – 122.
40. *Glendening E.D., Reed A.E., Carpenter J.E. et al.* NBO, Version 3.1., 2006.
41. *Oboyle N.M., Tenderholt A.L., Langner K.M.* // J. Comput. Chem. – 2008. – **29**. – P. 839 – 845.
42. *Parr R.G., Donnelly R., Levy M., Palke W.E.* // J. Chem. Phys. – 1978. – **68**. – P. 3801 – 3808.